Edge Contact Angle, Capillary Condensation, and Meniscus Depinning

Alexandr Malijevský
Department of Physical Chemistry, University of Chemical Technology Prague, Praha 6, 166 28, Czech Republic and The Czech Academy of Sciences, Institute of Chemical Process Fundamentals, Department of Molecular Modelling, 165 02 Prague, Czech Republic

Andrew O. Parry
Department of Mathematics, Imperial College London, London SW7 2BZ, United Kingdom

(Received 18 May 2021; accepted 12 August 2021; published 8 September 2021)

We study the phase equilibria of a fluid confined in an open capillary slit formed when a wall of finite length H is brought a distance L away from a second macroscopic surface. This system shows rich phase equilibria arising from the competition between two different types of capillary condensation, corner filling and meniscus depinning transitions depending on the value of the aspect ratio $a = L/H$. For long capillaries, with $a < 2/\pi$, the condensation is of type I involving menisci which are pinned at the top edges at the ends of the capillary characterized by an edge contact angle. For intermediate capillaries, with $2/\pi < a < 1$, depending on the value of the contact angle the condensation may be of type I or of type II, in which the menisci overspill into the reservoir and there is no pinning. For short capillaries, with $a > 1$, condensation is always of type II. In all regimes, capillary condensation is completely suppressed for sufficiently large contact angles. We show that there is an additional continuous phase transition in the condensed liquidlike phase, associated with the depinning of each meniscus as they round the upper open edges of the slit. Finite-size scaling predictions are developed for these transitions and phase boundaries which connect with the fluctuation theories of wetting and filling transitions. We test several of our predictions using a fully microscopic density functional theory which allows us to study the two types of capillary condensation and its suppression at the molecular level.

DOI: 10.1103/PhysRevLett.127.115703

The contact angle θ is central to the study of fluid adsorption and plays a crucial role in a number of surface phase transitions where it specifies the phase boundary [1–3]. For example, it vanishes at a wetting transition [4,5] and also determines that a right-angle corner is filled by liquid when $\theta < \pi/4$ [6,7]. It also appears in the macroscopic Kelvin equation for the pressure shift from saturation, $\delta p_{cc} = 2\gamma \cos\theta/L$, where γ is the interfacial tension, at which a vapor confined between two identical plates separated by a distance L, condenses to liquid [8,9]. If the walls are materially different, this generalizes immediately to $\delta p_{cc} = \gamma(\cos\theta_1 + \cos\theta_2)/L$, with θ_1 and θ_2 the corresponding contact angles. There are well-known cases where the equilibrium value of θ is modified by interfacial pinning, e.g., on rough surfaces where the modification is described by Wenzel's law [10] and is believed to underline the phenomena of contact angle hysteresis [11]. Interfacial pinning is also important for condensation in open capillaries. In particular, recent studies of fluid equilibria in a slit of finite length have highlighted the role played by an *edge contact angle* which characterizes the menisci pinned at the ends, and which replaces θ in the Kelvin equation [12–14].

In this Letter, we study a fluid confined in a slit formed when a wall of length H is brought near a second, infinite surface. We show that due to a combination of interfacial phenomena, the phase behavior is extremely rich. In particular, there are two types of capillary condensation as well as a continuous interfacial transition which has not been identified previously. At all these phase boundaries, an equilibrium edge contact angle plays a crucial role. The possible phase diagrams fall into three universal classes depending on the aspect ratio $a = L/H$. The rounding of these transitions, occurring at the mesoscopic scale, is linked to the fluctuation theories of wetting and filling transitions although several aspects are observable at the truly microscopic level.

We begin with macroscopics and suppose that our system is in contact with a reservoir of gas at pressure p at a temperature T below that of the bulk critical point T_c. Translational invariance is assumed along the slit, and gravity is neglected which is valid, for molecular fluids, provided L is sub mm [10]. We anticipate that as p is increased, the fluid inside the capillary condenses to liquid before bulk saturation p_{sat} is reached. The liquidlike phase is characterized by two circular menisci, which must be located near the ends. Since the bottom wall is infinite, the menisci meet it at Young's contact angle θ but there are two possibilities for the upper part of each menisci. For

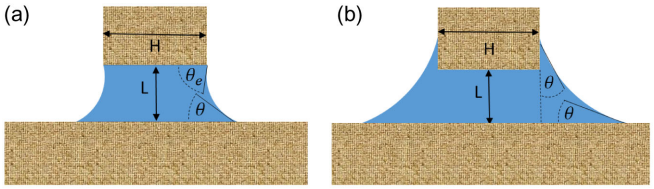

FIG. 1. Schematic illustration of two possible CL configurations in which the menisci (a) are pinned at the top corners with edge contact angle θ_e or (b) spill out of the slit meeting the walls with Young's contact angle θ.

example, they may be pinned at the edges, making an angle θ_e with respect to the horizontal [see Fig. 1(a)]. This edge contact angle is pressure dependent for any capillary-liquid phase (CL) but takes a specific value $\theta_e^{\rm cc}$ at the first-order transition where it coexists with the capillary-gas phase (CG); we refer to this as type I capillary condensation. Alternatively, the menisci may be unpinned, sitting outside the open ends touching the walls with the contact angle θ [see Fig. 1(b)]; we refer to this as type II capillary condensation.

The edge contact angle of any CL is determined geometrically by $L/R = \cos\theta + \cos\theta_e$ where $R = \gamma/\delta p$ is the Laplace radius and δp is the pressure difference across the meniscus which is approximately the deviation from $p_{\rm sat}$. The maximum value of the edge contact angle is $\theta_e^{\rm max} = \theta + \pi/2$, which is when the upper part of the menisci meet the vertical walls at Young's contact angle and are therefore unpinned. Balancing the grand potentials of the CG and CL phases taking into account only the volume and surface contributions shows that type I capillary condensation occurs when

$$\delta p_{\rm cc}^{I} = \frac{\gamma}{L}(\cos\theta + \cos\theta_e^{\rm cc}), \tag{1}$$

where $\theta_e^{\rm cc}$ is determined implicitly from

$$\cos^2\theta = \cos^2\theta_e^{\rm cc} + a\frac{\pi - \theta - \theta_e^{\rm cc} + \sin(\theta + \theta_e^{\rm cc})}{1 + a\tan(\frac{\theta_e^{\rm cc} - \theta}{2})}. \tag{2}$$

The modified Kelvin equation (1) is therefore of the same form as that for an infinite slit with two materially distinct walls. When the slit is infinitely long we recover the standard Kelvin equation, since $\theta_e^{\rm cc} = \theta$. As we shorten the capillary, the value of $\theta_e^{\rm cc}$ increases, and the condensation occurs closer to $p_{\rm sat}$. The loci of type I condensation terminates in one of two ways. It ends if $\theta_e^{\rm cc} = \theta_e^{\rm max}$ when it becomes of type II and no longer involves pinned menisci. Again, balancing the macroscopic contributions to the grand potentials of the CG and CL phases determines that this type of condensation occurs at the pressure shift

$$\delta p_{\rm cc}^{II} = \frac{2\gamma}{L}\frac{a[\cos\theta - \sin\theta + (\theta - \frac{\pi}{4})\sec\theta]}{a - 1 + \sqrt{1 + a^2 - 2a(\frac{\pi}{4}\sec^2\theta - \tan\theta)}}. \tag{3}$$

The numerator is positive only for $\theta < \pi/4$ implying that type II condensation can only occur in the complete corner filling regime. Alternatively, type I condensation ends when $\theta_e^{\rm cc} = \pi - \theta$, for which $\delta p_{\rm cc}^{I} = 0$. From Eq. (2) it follows that this occurs when the aspect ratio is $a_0 = \cot\theta$. We find it remarkable that the capillary condensation at this terminus of type I condensation mimics the phase separation in an infinite slit where the walls are materially different with opposing wetting properties, i.e., $\theta_2 = \pi - \theta_1$ [15]. Capillary condensation is suppressed for shorter capillaries.

We can summarize these results using simple phase diagrams, as shown in Fig. 2. We begin by classifying the capillaries according to their aspect ratio:

Long capillaries.—For $a < 2/\pi$, only type I condensation occurs up to a maximum value of the contact angle $\theta_0 = \cot^{-1} a$. For $\theta \geq \theta_0$ the gas inside the slit and the surrounding reservoir both condense to liquid at $p_{\rm sat}$. In addition, there is a line of meniscus depinning transitions when

$$\delta p_{\rm md} = \frac{\gamma(\cos\theta - \sin\theta)}{L}, \tag{4}$$

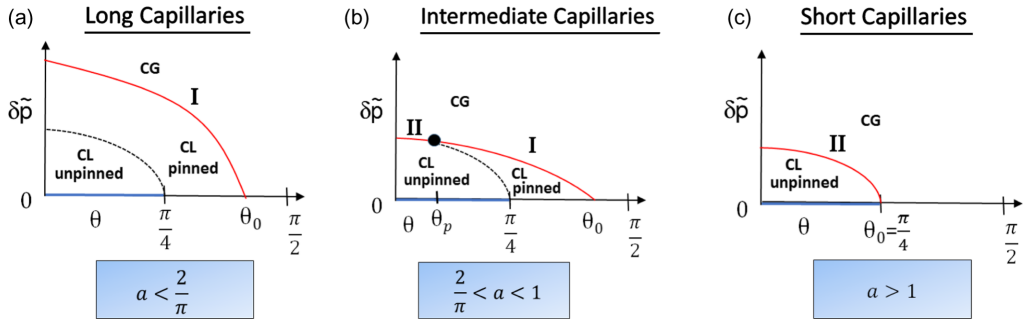

FIG. 2. Macroscopic phase diagrams for long, intermediate, and short capillaries showing the location of type I and type II condensation (red line), the meniscus depinning transition (dashed line), and the suppression of capillary condensation for different values of the aspect ratio. Here $\tilde{\delta}p = L\delta p/(2\gamma)$ is a dimensionless measure of the deviation from bulk saturation.

extending to the corner filling phase boundary $\theta = \pi/4$. On increasing the pressure from $\delta p_{\rm cc}^{I}$ the edge contact angle increases until it reaches $\theta_e = \theta_e^{\rm max}$, at which point the meniscus depins. This is shown as the dashed line in Fig. 2(a) and separates the regimes where the upper parts of the menisci are pinned or unpinned. Meniscus depinning is a continuous phase transition which is third-order for complete wetting and second-order for partial wetting. For example, for complete wetting, the third derivative of the grand potential, $\partial^3\Omega/\partial R^3$, has a discontinuity γ/L^2 associated with a singularity in the adsorption $\Gamma_{\rm sing} \propto (\delta p_{\rm md} - \delta p)^2$, which arises from the different qualitative structure of the meniscus in the pinned and the unpinned regimes. Finally the (blue) line, $0 < \theta < \pi/4$, at bulk saturation represents the line of complete corner filling. On approaching this line the adsorption diverges as $\Gamma \propto R^2$ due to the continuous growth of two menisci which have spilled out into the right-angle corners at each end of the slit.

Intermediate capillaries.—If $2/\pi < a < 1$, then condensation is of type II for $0 < \theta < \theta_p$ and type I for $\theta_p < \theta < \theta_0$. The crossover occurs when $a = \cos(2\theta_p)/(\pi/2 - 2\theta_p)$, at which $\theta_e^{\rm cc} = \theta_e^{\rm max}$, i.e., where meniscus depinning meets capillary condensation. Meniscus depinning only occurs in the range $\theta_p < \theta < \pi/4$ since for smaller contact angles the CL is metastable. As the aspect ratio approaches unity both θ_p and θ_0 approach $\pi/4$ (from different sides) and the lines of type I condensation and meniscus depinning vanish.

Short capillaries.—If the aspect ratio $a > 1$ only type II capillary condensation occurs up to the corner filling phase boundary with $\theta_0 = \pi/4$ beyond which capillary condensation is suppressed.

An alternative way of representing these macroscopic predictions is in terms of phase diagrams which are qualitatively different for the regimes corresponding to complete corner filling ($\theta < \pi/4$) and partial corner filling ($\theta > \pi/4$) (see Fig. 3 and the caption for details).

Some of these macroscopic predictions are slightly modified when we allow for thermal fluctuations. Since the capillary is pseudo one-dimensional all capillary condensation transitions are rounded occurring over a pressure range $\Delta p_{\rm cc} \propto \exp(-\beta\gamma LH)$ where the factor γLH is the approximate free-energy cost of phase separating the CG and CL along the capillary [16]. Such rounding is only of significance in the near vicinity of the (pseudo) capillary critical temperature which itself occurs when the smallest of the dimensions L or H is of order of the bulk correlation length. The meniscus depinning transition is also rounded. We consider the case of complete wetting first where the rounding is largest. At a macroscopic level meniscus depinning occurs when $R = L$, i.e., when a quarter circular meniscus just fits into the open ends of the capillary. However, this ignores the presence of the complete wetting layers along the bottom and vertical walls which are characterized by a thickness ℓ_π and also a parallel correlation length $\xi_\parallel$ arising from thermal interfacial fluctuations [2]. These length scales soften the effective slit width, with depinning occurring when $R \approx L - \ell_\pi \pm \xi_\parallel$. Allowing for the pressure dependence of the parallel correlation length, $\xi_\parallel \approx \delta p^{-\nu_\parallel^{\rm co}}$, implies that for complete wetting the meniscus depinning transition is rounded over the pressure range $\Delta p_{\rm md} \propto L^{\nu_\parallel^{\rm co}-2}$ and the type I-II crossover over the aspect ratio range $\Delta a_p \propto L^{\nu_\parallel^{\rm co}-1}$. For systems with dispersion forces, $\nu_\parallel^{\rm co} = 2/3$ [17], implying that $\Delta p_{\rm md} \propto L^{-(4/3)}$ and $\Delta a_p \propto L^{-(1/3)}$. Similar considerations apply for partial wetting; however, in this case $\xi_\parallel$ remains finite leading to the universal finite-size scaling predictions $\Delta p_{\rm md} \propto L^{-2}$ and $\Delta a_p \propto L^{-1}$. The macroscopic predictions are also

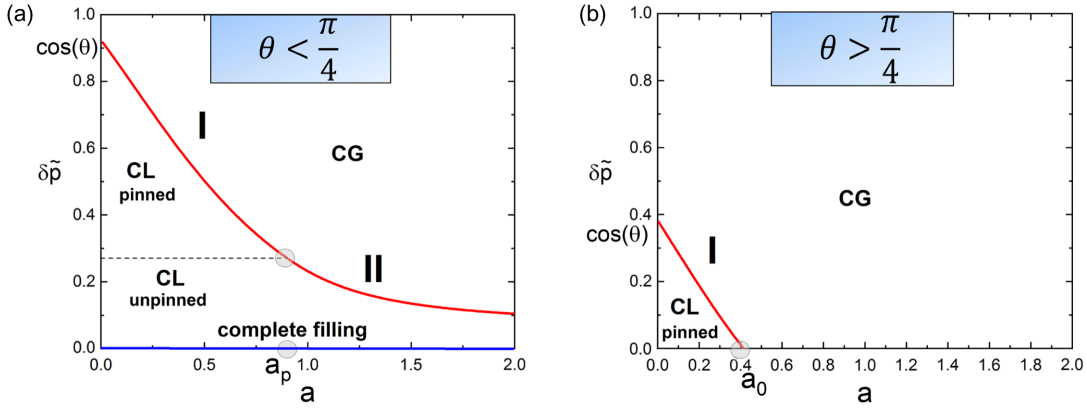

FIG. 3. Macroscopic phase diagrams for complete and partial corner filling. For $\theta < \pi/4$ (a) both type I and type II condensation (red line) occur in addition to meniscus depinning (dashed line) and complete corner filling (blue line). The type I-II crossover occurs at $a_p = \cos(2\theta)/(\pi/2 - 2\theta)$. As θ increases to $\pi/4$ the lines of meniscus depinning and type II condensation merge into the saturation curve and disappear. For $\theta > \pi/4$ (b) only type I condensation exists and is suppressed when the aspect ratio is larger than $a_0 = \cot\theta$.

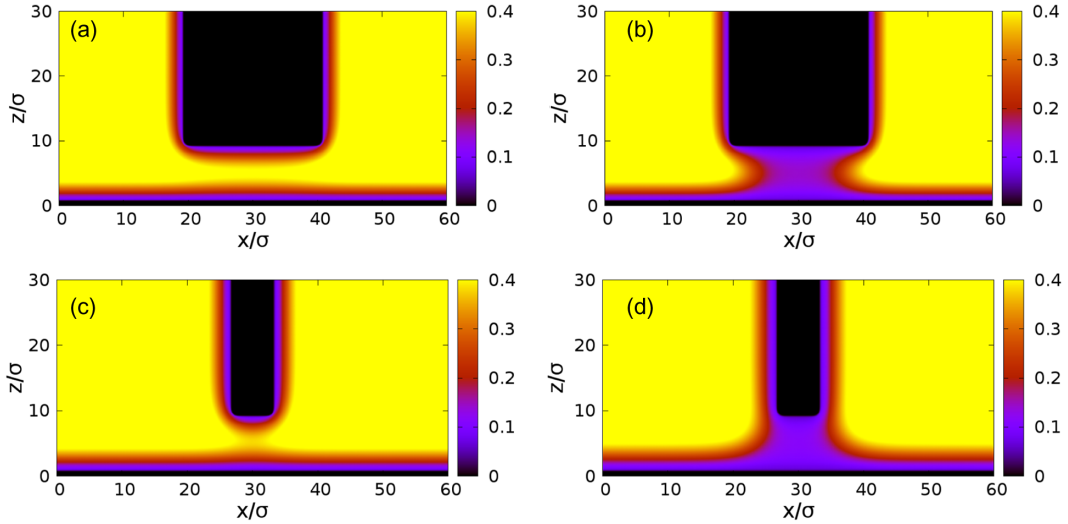

FIG. 4. Type I and type II condensation in a microscopic slit with repulsive walls and width $L = 10\sigma$. The plots (a) and (b) show the coexisting CL and CG phases for aspect ratio $a = 1/2$, while (c) and (d) are the coexisting CL and CG phases for $a = 1$.

modified slightly if the corner filling transition at $\theta = \pi/4$ is continuous. Macroscopically, the loci of the meniscus depinning transitions (for $a < 1$) and line of type II condensation (for $a > 1$) end exactly at $\theta = \pi/4$. If the right-angle corners show continuous corner filling, however, these transitions end when $\theta - \pi/4 \propto L^{-1/\beta_w}$. Here, β_w is the critical exponent describing the thickness, $\ell_w \propto (\theta - (\pi/4))^{-\beta_w}$, of the adsorbed layer of liquid at a right-angle corner at $p = p_{\mathrm{sat}}$ [18], i.e., a meniscus must be present whenever the mesoscopic thickness of the adsorbed liquid is greater than the slit width. For systems with dispersion forces this implies that meniscus depinning slightly extends into the partial filling regime until $\theta - (\pi/4) \propto L^{-2}$.

We have compared our predictions with a microscopic density functional theory (DFT) model which allows us to study these phenomena at the molecular scale [19]. We begin by showing that for complete wetting, the capillary condensation is type I and type II for small and large aspect ratios, respectively. We employ the same DFT model that we have used recently [13] which combines Rosenfeld's fundamental measure theory [20] accurately describing any packing effects, with a mean-field treatment of the attractive part of the interatomic interaction modeled by a truncated Lennard-Jones (LJ) potential. See the Supplementary Material for details [21]. Actually, we flip the scenario and consider walls which have a purely long-ranged repulsive component, which ensures that they are completely dry with contact angle $\theta = \pi$, focusing on the character of the capillary evaporation as the pressure is *reduced* to p_{sat} (that is the roles played by the CG and CL phases are simply reversed). We have determined the line of capillary condensation over a wide range of the aspect ratio for a microscopic slit separation $L = 10\sigma$, with σ the molecular diameter [21]. Figures 4(a) and 4(b) show the coexisting CL and CG phases for aspect ratio $a = 1/2$, illustrating type I condensation, while Figs. 4(c) and 4(d) show the coexisting phases for $a = 1$, illustrating type II condensation.

Finally, we show that for $\theta > \pi/4$ condensation is only of type I and is suppressed for aspect ratios $a > a_0$, which we compare with the theoretical prediction $a_0 = \cot\theta$. We add an attractive part to the substrate-fluid potential in order to decrease the contact angle assuming the walls are made of atoms interacting with the fluid via a full LJ potential. We set the temperature $T = 0.85T_c$, for which the contact angle $\theta \approx 53°$ [23]. As predicted, the phase diagram shows only a line of type I capillary condensation which terminates at $a_0 \approx 0.78$, which is extremely close to the macroscopic prediction $a_0 \approx 0.75$ (Fig. 5). Representative density profiles of the coexisting states (for $H = 15\sigma$), for which $a = 2/3$, are also shown and illustrate how the meniscus pinning is mimicking the properties of condensation between two walls with opposing wetting properties, i.e, $\theta_e^{\mathrm{cc}} \approx \pi - \theta$.

In summary, we have shown that in an open slit geometry the capillary condensation may occur in two different ways involving pinned or unpinned menisci separated by a continuous meniscus depinning transition. The phase boundaries are determined by the values of an edge contact angle somewhat analogous to how the Young contact angle determines the phase boundary for wetting and filling transitions. The resulting phase diagrams fall into one of three possible universal classes depending on the slit aspect ratio. The richness of the possible phase behavior emerges from the interplay between different interfacial phenomena and are connected to the fluctuation theory of fundamental surface phase transitions. The distinction between type I and type II condensation and the presence of meniscus depinning transitions will occur in other geometries which

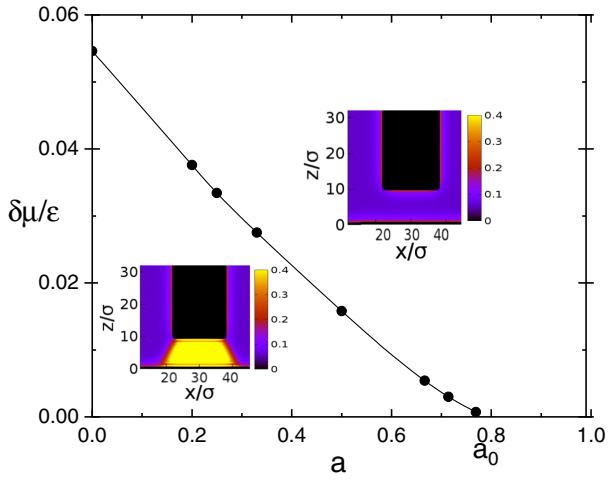

FIG. 5. Phase diagram for partial corner filling, with $\theta \approx 53°$ showing a line of type I capillary condensation ending at bulk saturation when the aspect ratio $a_0 \approx 0.78$, close to the macroscopic prediction $a_0 \approx 0.75$. Here $\delta\mu/\varepsilon$ is a measure of the chemical potential deviation from saturation measured in units of fluid-fluid potential. Coexisting density profiles for $a = 2/3$ are shown.

are certainly experimentally accessible, for example, when a vertical cylinder is brought into close contact with a flat surface. The rounding of the meniscus transition considered here arises due to the thermal fluctuations of the adsorbed wetting layers and occurs for even perfectly sharp geometries. It would also be interesting to understand how surface roughness affects the edge contact angle and the meniscus depinning transition, which may well connect with the phenomena of contact angle hysteresis. Including gravity may also introduce interesting new effects associated with capillary emptying transitions [24,25]. Finally, the equilibrium phase transitions considered here are also a prerequisite for understanding the dynamics of meniscus depinning which may be studied, for example, using dynamical DFT or simulation methods similar to those described in [26].

This work was financially supported by the Czech Science Foundation, Project No. GA 20-14547S.

[1] J. S. Rowlinson and B. Widom, *Molecular Theory of Capillarity* (Oxford University Press, Oxford, 1982).
[2] S. Dietrich, in *Phase Transitions and Critical Phenomena*, edited by C. Domb and J. L. Lebowitz (Academic Press, New York, 1988), Vol. 12.
[3] D. Bonn, J. Eggers, J. Indekeu, J. Meunier, and E. Rolley, Rev. Mod. Phys. **81**, 739 (2009).
[4] J. W. Cahn, J. Chem. Phys. **66**, 3667 (1977).
[5] C. Ebner and W. F. Saam, Phys. Rev. Lett. **38**, 1486 (1977).
[6] E. H. Hauge, Phys. Rev. A **46**, 4994 (1992).
[7] K. Rejmer, S. Dietrich, and M. Napirkówski, Phys. Rev. E **60**, 4027 (1999).
[8] S. J. Gregg and K. S. W. Sing, *Adsorption, Surface Area and Porosity* (Academic, New York, 1982).
[9] R. Evans and U. Marini Bettolo Marconni, Chem. Phys. Lett. **114**, 415 (1985).
[10] P. de Gennes, F. Brochard-Wyart, and D. Quèrè, *Capillarity and Wetting Phenomena: Drops, Bubbles, Pearls, Waves* (Springer, New York, 2013).
[11] D. Quèrè, Annu. Rev. Mater. Res. **38**, 71 (2008).
[12] A. Malijevský, A. O. Parry, and M. Pospíšil, Phys. Rev. E **96**, 020801(R) (2017).
[13] M. Láska, A. O. Parry, and A. Malijevský, Phys. Rev. Lett. **124**, 115701 (2020).
[14] Q. Yang, P. Z. Sun, L. Fumagalli, Y. V. Stebunov, S. J. Haigh, Z. W. Zhou, I. V. Grigorieva, F. C. Wang, and A. K. Geim, Nature (London) **588**, 250 (2020).
[15] A. O. Parry and R. Evans, Phys. Rev. Lett. **64**, 439 (1990).
[16] V. Privman and M. E. Fisher, J. Stat. Phys. **33**, 385 (1983).
[17] R. Lipowsky, Phys. Rev. B **32**, 1731 (1985).
[18] A. O. Parry, C. Rascón, and A. J. Wood, Phys. Rev. Lett. **85**, 345 (2000).
[19] R. Evans, Adv. Phys. **28**, 143 (1979).
[20] Y. Rosenfeld, Phys. Rev. Lett. **63**, 980 (1989).
[21] See Supplemental Material at http://link.aps.org/supplemental/10.1103/PhysRevLett.127.115703 for details of the DFT model, which includes Ref. [22].
[22] A. Malijevský, J. Phys. Condens. Matter **25**, 445006 (2013).
[23] A. Malijevský and A. O. Parry, Phys. Rev. **91**, 052401 (2015).
[24] A. O. Parry, C. Rascón, E. A. G. Jamie, and D. G. A. L. Aarts, Phys. Rev. Lett. **108**, 246101 (2012).
[25] C. Rascón, A. O. Parry, and D. G. A. L. Aarts, Proc. Natl. Acad. Sci. U.S.A. **113**, 12633 (2016).
[26] M. L. Trobo, E. V. Albano, and K. Binder, J. Chem. Phys. **148**, 114701 (2018).